Domain configuration and magnetization switching in arrays of permalloy nanostripes

Ó Iglesias-Freire[1], M Jaafar[1,2], L Pérez[3], O de Abril[4], M Vázquez[1] and A Asenjo[1]

[1] Instituto de Ciencia de Materiales de Madrid, CSIC, Sor Juana Inés de la Cruz, 3, Madrid 28049

[2] Dpto. Física de la Materia Condensada, Universidad Autónoma de Madrid, Cantoblanco 28049

[3] Dpto. Física de Materiales, Universidad Complutense de Madrid, Madrid 28040

[4] Dpto. Física e Instalaciones Aplicadas a la Edificación, al Medio Ambiente y al Urbanismo, Universidad Politécnica de Madrid, Madrid 28040

E-mail: aasenjo@icmm.csic.es

Abstract:

The proximity effect in the collective behavior of arrays of magnetic nanostripes is currently a subject of intensive research. The imperative of reducing the size and distances between elements in order to achieve higher storage capacity, faster access to the information as well as low energy consumption, brings consequences about the isolated behavior of the elements and devices. Parallel to each other permalloy nanostripes with high aspect ratio have been prepared by nanolithography technique. The evolution of the closure domains and the magnetization direction in individual nanostructures has been imaged under applied magnetic fields using Variable Field Magnetic Force Microscopy. Moreover, the magnetostatic interactions between neighboring elements and the proximity effects in arrays of such nanostructures have been quantitatively analyzed by Magnetic Force Microscopy and micromagnetic simulations. The agreement between simulations and the experimental results allows us to conclude the relevance of those interactions depending on the geometry characteristics. In particular, results suggest that the magnetostatic coupling between adjacent nanostripes vanishes for separation distances higher than 500nm.

1. Introduction

The observation of spin dependent phenomena in the transport properties of ferromagnetic materials has been of crucial importance in the improvement of ultra-high density magnetic data storage systems. The observation of giant magnetoresistance in multilayered thin films [1],[2] the spin valve effect [3] and the tunnel magnetoresistance [4] has enabled to multiply the capacity of hard disk drives and also to develop non volatile magnetic-based random access memories (M-RAM) [5]. All these phenomena and devices constitute the core of a new branch of Electronics called Magnetoelectronics or Metal Spintronics. All these devices, hard disks and MRAMs, are based on the information storage in independent magnetic units, bits or tunnel junctions respectively. In the last few years, new devices have been proposed, based on a completely different concept: information would be storaged in domain walls of ferromagnetic nanostripes in two new different architectures: domain wall logic [6] and racetrack-memories [7]. In this framework, the study of domain walls in permalloy ($Ni_{80}Fe_{20}$) nanostripes has gained considerable interest in the last few years. Due to its magnetic properties (i.e., large magnetic moment together with vanishing both magnetostriction and magnetocrystalline anisotropy resulting in ultrasoft magnetic behavior and very low coercivity), Permalloy is an excellent playground to test the features of these new devices.

Plenty of literature can be found regarding dynamic magnetization processes [8],[9],[10], domain wall pinning and propagation [11],[12],[13],[14] and magnetization switching processes [15],[16],[17],[18],[19] of permalloy nanowires and nanostripes. Up to now, almost all the studies have been focused on the behavior of a single nanostripe or in a small collection of them whereas in real devices, high density of nanowires should be used in order to reach high storage density. When nanostripes are placed close to each other, the magnetic state of each nanostripe can affect that of its neighbors via magnetostatic interactions. Some studies can be found on the magnetic interactions between neighboring stripes on different materials as cobalt [20],[21],[22], nickel [23],[24], iron [25] or Fe_3Pt [26]. In these studies, the magnetic properties of cylindrical nanowires embedded on a nanoporous alumina membrane are mostly studied and the magnetic behavior is extracted from measurements in arrays of nanowires, using bulk magnetometry techniques, such as vibrating sample magnetometer (VSM) or superconducting quantum interference device SQUID, which yield averaged information over a macroscopic region. When dealing with nanostructures, this kind of measurement encompasses multitude of elements, making harder to reach a full understanding of the magnetization reversal process of each element individually. Magneto-optical Kerr effect (MOKE) magnetometry can be alternatively used as a local technique but its resolution is limited to the micrometric range. Hysteresis loops on individual nanostructures [27] and arrays of them [28] have already been studied by means of Variable Field Magnetic Force Microscopy (VF-MFM). Micromagnetic

simulations performed with the Object Oriented Micromagnetic Framework code (OOMMF) [29] have also been utilized, being a valuable tool to adequately interpret the measurements.

2. Experimental

An array of permalloy nanostripes was grown by a combination of electron beam lithography (EBL), sputtering and lift-off processes, using silicon wafers as substrates. The nanostripes are 25 nm thick, 100 nm wide and 5 μm long. Both lateral and longitudinal distances between neighboring stripes are 500 nm.

The experimental characterization was performed at room temperature using a VF-MFM [30] from *Nanotec Electrónica*, under in plane magnetic fields applied either parallel or perpendicular to the main axis of the nanostructures. The same commercial Nanosensors PPP-LM-MFMR (k=3 N/m, f_0=75 kHz) tip was used throughout the experiments.

Aiming for an accurate interpretation of the experimental results, micromagnetic simulations were carried out using the OOMMF code, using standard Permalloy parameters (M_S=8.6·10^5 A/m, A=13·10^{-12} J/m, k1=0). The black (white) background contrast in the simulations stands for a negative (positive) divergence of the magnetization. This should yield analogous information compared to an MFM image, where the contrast actually arises from the axial field lines emerging wherever the sample magnetization diverges locally. Coloured arrows are also plotted, representing the local orientation of the magnetization. In this case, red (blue) coloured arrows stand for a negative (positive) z-component of the local magnetization.

3. Results and discussion

The high aspect ratio of the nanostripes is observed in the topographic image shown in figure 1.a. The MFM picture in figure 1.b was obtained in the remanent state, after saturating the sample parallel to the easy axis. A weak contrast is recorded along the stripes due to the single domain configuration, whereas the large divergence of the magnetization at the stripe ends causes a stronger interaction with the MFM tip (figure 1.c). MFM images in figure 1 show all of the stripes with their magnetization pointing along the shape-induced easy axis, parallel to each other, suggesting that a low magnetostatic coupling between neighboring stripes is present, since no influence in the magnetic state of the surrounding nanostructures is seen. In order to gain insight into such coupling, series of MFM experiments were carried out under external

fields applied whether along the easy (longitudinal) or the hard (transversal to the longitudinal one) axis.

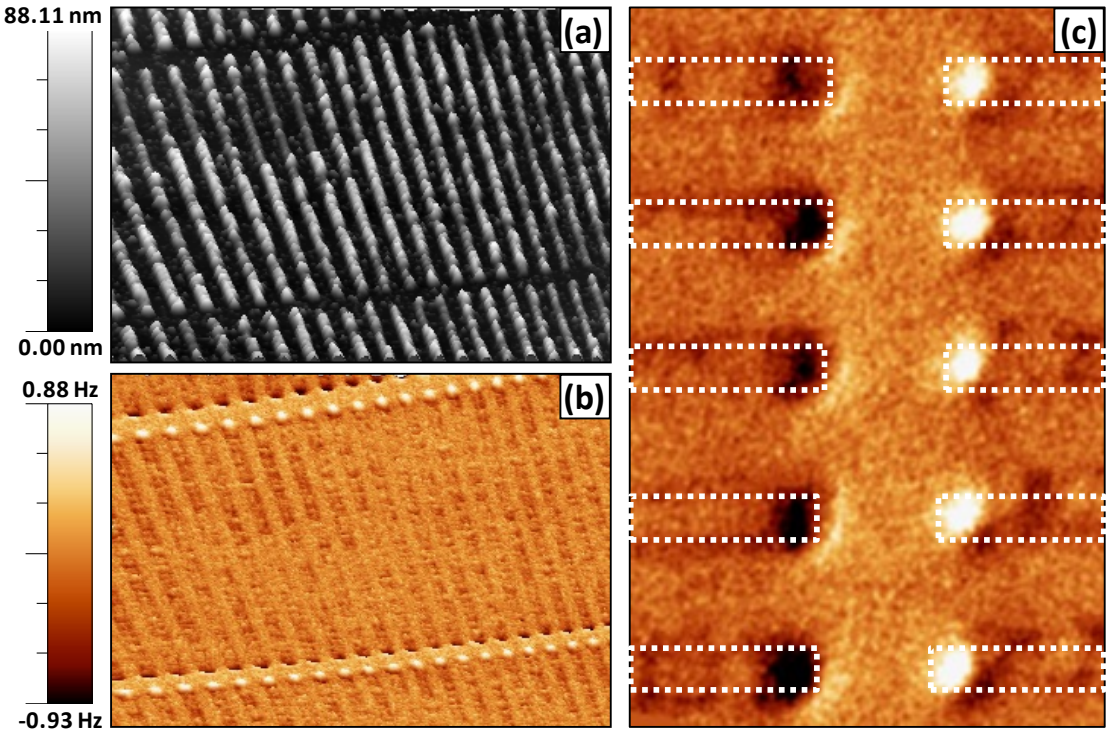

Figure 1. (a) Topography and (b) MFM image in the remanent state after saturation along the main axis of the stripes. Images size 10 µm × 7 µm. (c) Zoom in on (b), image size 1.6 µm × 2.4 µm

The magnetization reversal process along the in-plane hard axis is presented in figure 2. Figure 2.a shows the remanent state after ex-situ saturation with 1 Tesla along the vertical direction in the images (see black arrow). The strong shape anisotropy causes the magnetization at remanence to point along the easy axis direction, forming a single domain configuration. In the case of perfectly symmetric stripes, there would be no preferential polarity for the single domains at remanence. However, every single misalignment of the external field will break the symmetry of the energy landscape and cause most of the domains to point along the same direction. We believe this is the reason why most of the stripes in figure 2.a have a parallel magnetization. In addition, a small misalignment of the in-situ magnetic field applied during the experiment is expected.

The contrast at the ends of the nanostructures becomes asymmetric under applied fields due to the development of closure domains (see figure 2.c). Furthermore, as the field is increased this contrast decreases significantly (see figure 2.d). Gradually, the magnetization rotates away from the longitudinal axis and a dipolar contrast can be observed along the hard axis for large magnetic fields (figures 2.e and 2.f). For a proper interpretation of the magnetization reversal process, we should be aware that the contrast in the images can also be influenced by eventual

changes in the magnetization of the MFM sensing tip at high fields [31]. In particular, when imaging at relatively high fields it is crucial to rule out eventual contrast contributions caused by changes in the magnetization orientation of the tip. The hysteresis loop of the MFM probe used throughout these experiments was performed by imaging a hard disk sample while sweeping the external field. No significant change was found in the magnetic configuration at the tip apex, apart from a slight tilt of its magnetization, under the maximum field used in the experiments.

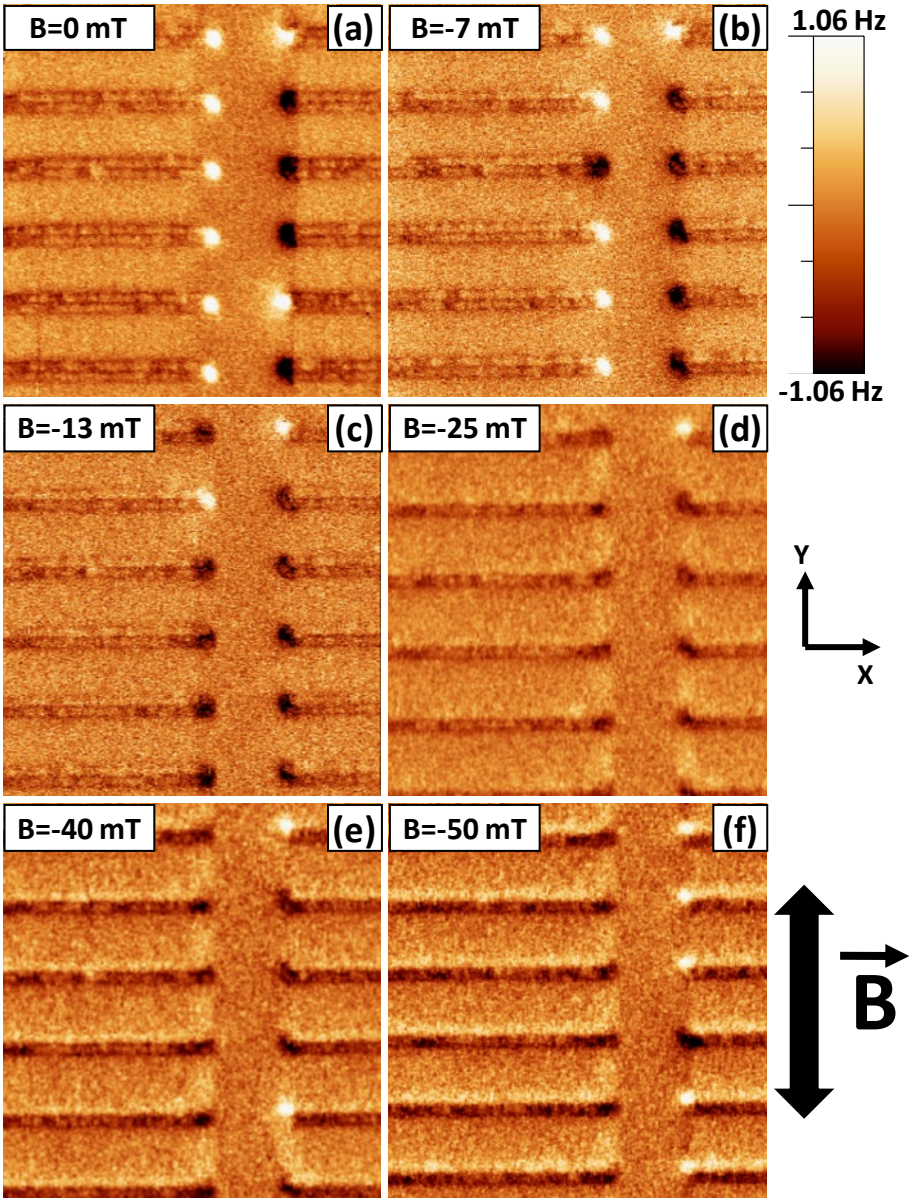

Figure 2. Sequence of (3 µm × 3 µm) MFM images obtained under different magnetic fields applied along the hard-axis.

In order to clarify the evolution of the contrast observed in the MFM pictures, we simulated the magnetic behavior of a single nanostripe with similar dimensions to the experimental ones. Next figure shows the equilibrium magnetization distribution under different fields applied whether

along its hard or easy axis. Note that, in the first case (fig. 3.a), a small misalignment was introduced in the saturating field, compared to the hard axis. Therefore, in order to break the symmetry of the system, a field component of 0.1 mT was applied along the easy axis when saturating the sample and removed thereafter. As a result, switching off the field lets the spins turn back to their easy axis (with a polarity defined by this 0.1 mT component), giving rise to an intense contrast at the ends of the stripes caused by closure domains. These closure domains evolve as the external field increases until a dipolar contrast can be seen along the transversal direction, for large fields. Due to the considerable energy expense that is required for the system to get magnetized along the hard axis direction, just a weak contrast is observed experimentally (fig. 2.e and 2.f) for the maximum applied fields.

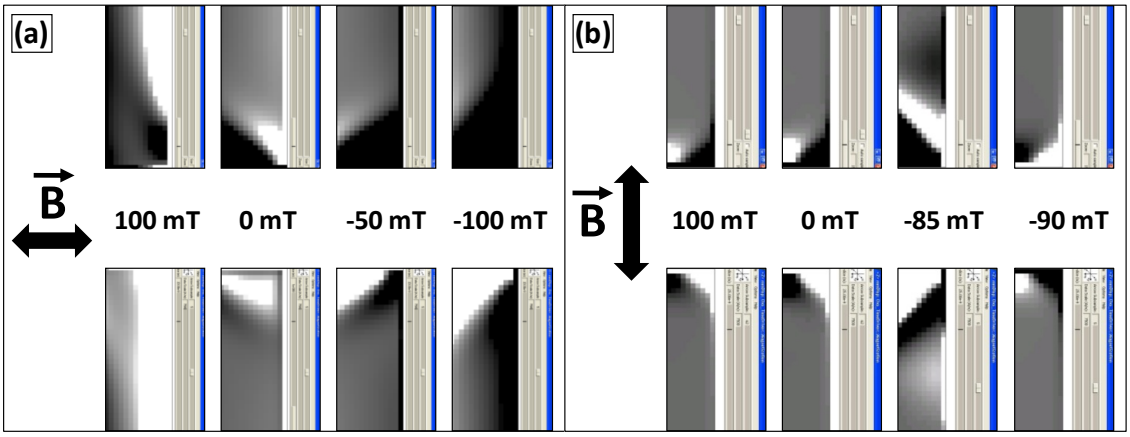

Figure 3. Micromagnetic simulation of the magnetization reversal process in a single permalloy nanostripe (5 μm x 100 nm x 25 nm). For clarity reasons, only both ends of the same stripe are shown. (a) When large external fields are applied along its hard axis, a transversal dipolar contrast is observed all along the stripe. For small fields, closure domains are seen at both ends. (b) Closure domains are also formed at the ends, when an external field close to the switching field is applied along the easy axis direction.

In the case of magnetic fields applied along the easy axis (figure 3.b), the nanostructure presents a single domain configuration for a large range of fields, including remanence, with the characteristic dark-bright contrast at the ends of the stripe. However, closure domains are formed close to the switching field, before two 180º domain walls nucleate at both ends and propagate along the stripe. Thus, these nanostripes reverse their magnetization abruptly by means of domain wall nucleation-propagation-annihilation processes, which are much faster than the scan speed of force microscopes and, therefore, out of our present scope. In figure 4, a series of MFM images obtained under magnetic fields applied along the easy axis is presented. A particular nanostructure has been highlighted as a guide for the eye in order to follow the collective evolution of the magnetic configuration of the whole array. Remarkably, no correlation was found between the magnetic state of one nanostructure and the one of its neighbors. On the one hand, the adjacent elements of a nanostripe can have their magnetization

pointing parallel or antiparallel, with no apparent preference. On the other hand, the elements placed in front of a stripe can also be magnetized parallel or antiparallel, as seen in fig. 4.

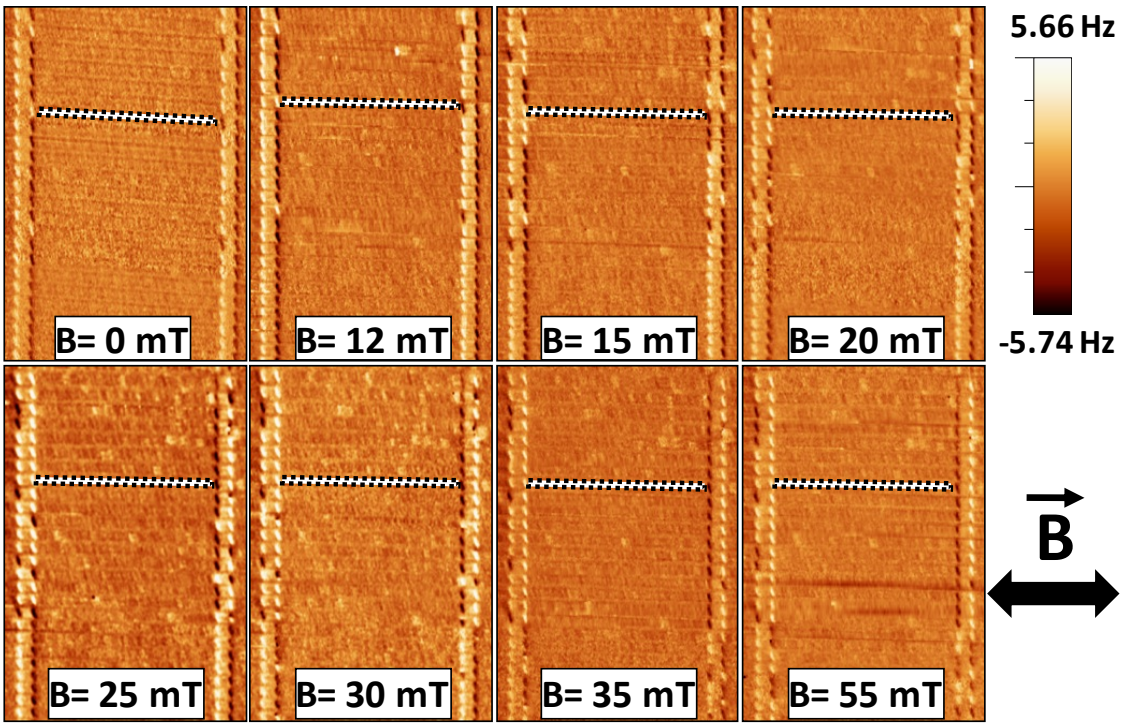

Figure 4. Sequence of (7 μm × 13 μm) MFM images obtained at different magnetic fields applied along the easy-axis of the nanostripes. A particular stripe has been highlighted, as a guide for the eye.

As seen above, experimental results are in good agreement with the simulated images in both configurations, so we can assume that the MFM contrast arises from the divergence of the magnetization in the sample. In the following, we will focus on the influence of neighboring nanostructures. In order to estimate what the critical distance might be, for which the magnetostatic interaction between neighbors becomes relevant and influence the magnetic behavior of the single elements, arrays of permalloy planar wires with variable separation distances were simulated. To achieve reasonable computation times, the length of these nanostripes has been reduced down to 1 μm, whereas both width and thickness were kept constant at 100 nm and 25 nm, respectively. Nevertheless, no significant difference on the magnetic behavior of individual nanostripes is expected, provided that we still keep a large aspect ratio. Both longitudinal and transversal separation distances among neighboring wires were varied, in order to estimate the critical length for which the dipole-dipole interaction becomes negligible. Although simulations with a large number of different distances were carried out, only the most significant cases are presented here.

For large enough distances, magnetization reversal processes taking place in each wire should be equivalent and analogous to those of an isolated single stripe. This is the case for stripes

whose separation distance is larger than around 500 nm (see graph in figure 5), where two 180º walls are nucleated at both stripe ends and propagate until they annihilate in the central region of every magnetic nanostructure (figure 5.a). By decreasing now the transversal separation (perpendicular to the stripe long axis) below this critical value, stripes are not independent anymore and prefer reversing their magnetization in groups. The first elements to switch their polarity are those placed at the ends of the array and once this process has started, it gradually spreads out to the neighboring nanostructures, as can be observed in the sequence in figure 5.b. Due to size restrictions in this paper, only two steps of the process are shown. However, stripes within each row reversed its magnetization one at a time, being those placed at the center of the image the last ones to do it.

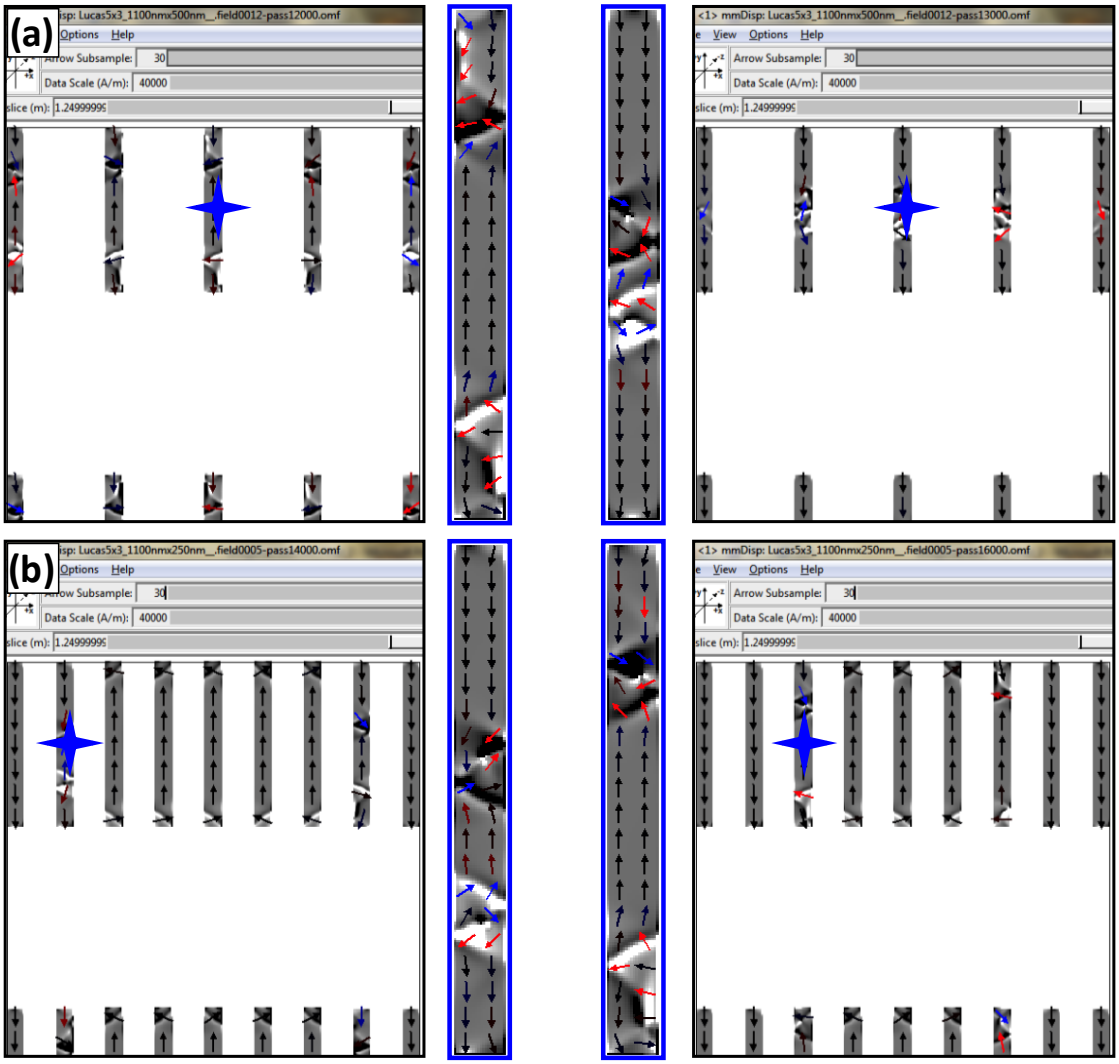

Figure 5. Simulated dynamic evolution of the magnetization reversal process in arrays of permalloy nanostripes (1 μm x 100 nm x 25 nm), for a constant longitudinal distance of 1100 nm, with the field applied along the easy axis. The transversal separation is (a) 500 nm and (b) 250 nm. Images show the dynamic evolution of the magnetization reversal process at the switching fields: (a) 96 mT and (b) 89 mT, applied downwards in the pictures, after saturation

upwards. Two 180º domain walls are nucleated in both sides of the stripes and propagate fast. For clarity, nanostripes highlighted with a blue cross are enlarged and shown right next to the simulation image.

In addition, the magnetostatic coupling along the longitudinal axis was checked. Stripes placed far enough from each other act as independent structures until the longitudinal separation decreases below 500 nm, where they start behaving as single elements with domain walls "jumping" between neighboring wires (figure 6.a). In this case, domain walls nucleate at the free ends of the outermost stripes and propagate inwards all along the wires until they annihilate at the opposite stripe side, inducing instantly the formation of a domain wall in the contiguous end of the neighboring nanostructure. Thus, domain walls "jump" from stripe to stripe, yielding every column of wires a single-element-like behavior.

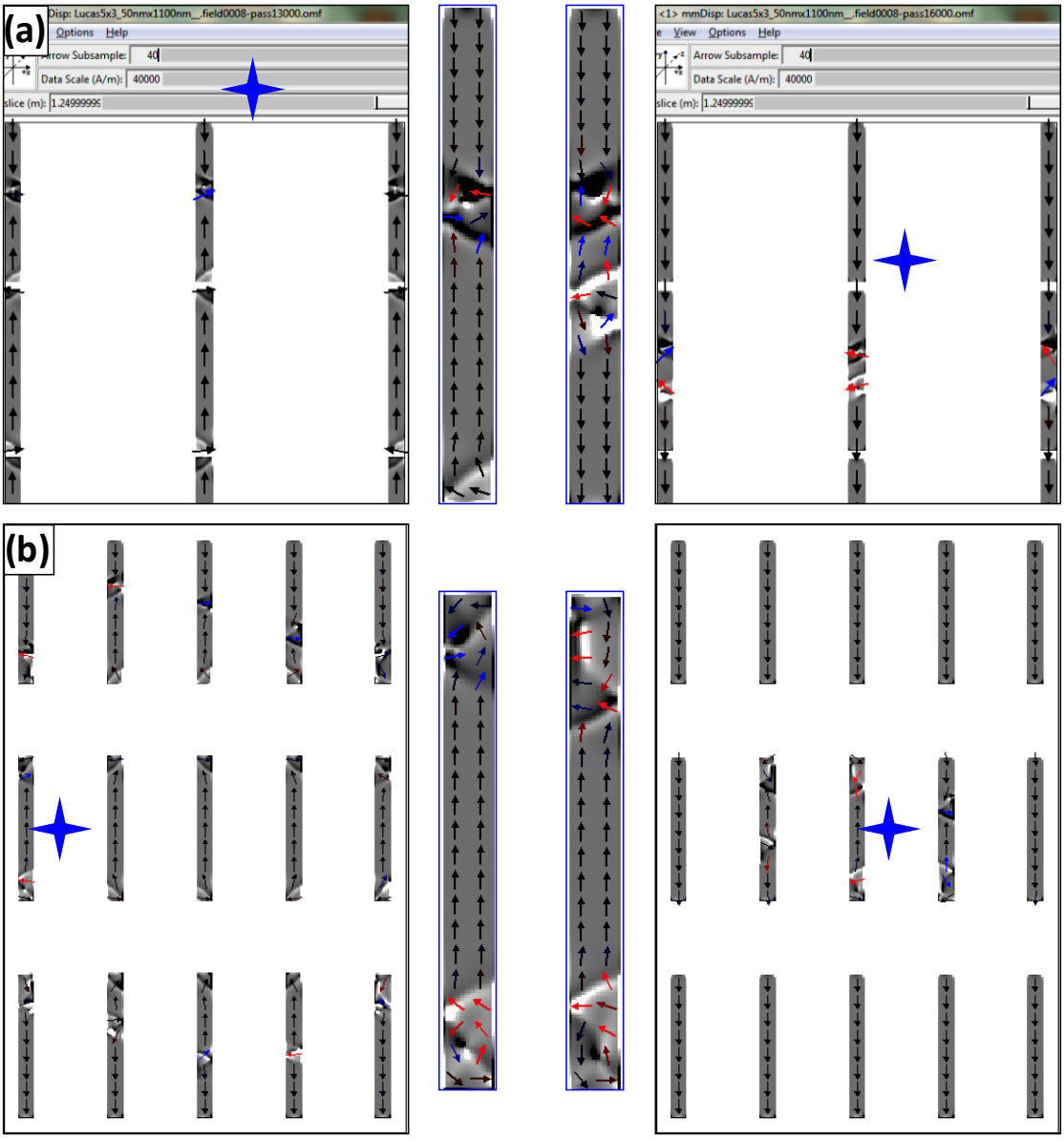

Figure 6. Simulated evolution over time of the reversal process for an applied field of (a) -92 mT and (b) -82 mT, along the easy axis. (a) Longitudinal (transversal) separation distances between stripes are 50 nm (1100 nm).

Columns of stripes behave as single structures, with domain walls nucleating at the free ends of the outermost stripes, propagating along them and "jumping" into neighboring nanostructures. (b) Both longitudinal and transversal separations are 500 nm, equivalent to the experimental case. A mixed behavior (see text) suggests that 500 nm is the critical length for the magnetostatic coupling between stripes.

Interestingly, the experimental case shown in the previous section lies in the boundary of an eventual magnetostatic coupling, as predicted by the simulations. The weakness of this coupling is reflected in figure 6.b, where a mixture of the explained scenarios can be observed. On the one hand, domain walls originate at the outermost edges, propagating and inducing the switching in the neighboring structures. On the other hand, these walls do not "jump" between stripes since, close before they reach the opposite end of the stripe, a second series of domain walls originates right there and start propagating to the opposite direction. This second set of walls is responsible for inducing the switching process in the neighboring wires. As a result, simulations suggest that 500 nm is the critical separation distance for the permalloy stripes to be magnetostatically coupled, both in the longitudinal and transverse directions.

4. Conclusions

The magnetization reversal process in arrays of high aspect ratio Permalloy nanostripes was investigated in parallel by magnetic force microscopy imaging and micromagnetic simulations. The following conclusions can be outlined: (i) as expected from the dominant longitudinal shape anisotropy, the stable remanent magnetic state of the stripes consists of an axial single domain structure. Applying external fields allows to observe the formation of closure domains; (ii) the separation distances between neighboring stripes (500 nm) is enough to overcome the magnetostatic coupling and avoid a multistripe character of the whole array; (iii) micromagnetic simulations predict the critical distance for the onset of magnetostatic coupling between neighboring elements to be around this distance, i.e. 500 nm; (iv) simulations predict stripes with a small longitudinal separation to behave as single elements, with domain walls nucleating at the outermost ends of the array, propagating and "jumping" between stripes.

5. Acknowledgments

We gratefully thank funding from projects CSD2010-00024, MAT2007-65420-c02-01, MAT2010-20798 (MINECO), MAT 2011-28751-C02-02 and S2009/MAT-1467 (CAM).

References

[1] Baibich M N, Broto J M, Fert A, Nguyen Van Dau F, Petroff F, Etienne P, Creuzet G, Friederich A and Chazelas J 1988 *Physical Review Letters* **61** 2472
[2] Binasch G, Grünberg P, Saurenbach F and Zinn W 1989 *Physical Review B* **39** 4828
[3] Dieny B, Speriosu V S, Parkin S S P, Gurney B A, Wilhoit D R and Mauri D 1991 *Physical Review B* **43** 1297
[4] Moodera J S, Kinder L R, Wong T M and Meservey R 1995 *Physical Review Letters* **74** 3273
[5] Gallagher W J and Parkin S S P 2006 *IBM Journal of Research and Development* **50** 5
[6] Allwood D A, Xiong G, Faulkner C C, Atkinson D, Petit D and Cowburn R P 2005 *Science* **309** 1688-1692
[7] Parkin S S P, Hayashi M and Thomas L 2008 *Science* **320** 190-194
[8] Zhang H, Song C and Wang P 2009 *Journal of Applied Physics* **105** 07E716
[9] Warnicke P, Nakatani Y, Kasai S and Ono T 2008 *Physical Review B* **78** 012413
[10] Gérardin O, Youssef J B and Le Gall H 2000 *Journal of Applied Physics* **88** 5899
[11] Atkinson D, Allwood D A, Xiong G, Cooke M D, Faulkner C C and Cowburn R P 2003 *Nature Materials* **2** 85
[12] Nakatani Y, Thiaville A and Miltat J 2003 *Nature Materials* **2** 521
[13] Petit D, Jausovec A-V, Zeng H T, Lewis E, O'Brien L, Read D and Cowburn R P 2009 *Physical Review B* **79** 214405
[14] Bogart L K, Eastwood D S and Atkinson D 2008 *Journal of Applied Physics* **104** 033904
[15] Tartakovskaya E V, Pardavi-Horvath M and Vázquez M 2010 *Journal of Magnetism and Magnetic Materials* **322** 743-747
[16] Zeng H T, Read D, Petit D, Jausovec A V, O'Brien L, Lewis E R and Cowburn R P 2009 *Applied Physics Letters* **94** 103113
[17] Atkinson D, Eastwood D S and Bogart L K 2008 *Applied Physics Letters* **92** 022510
[18] Hayashi M, Thomas L, Rettner C, Moriya R, Jiang X and Parkin S S P 2006 *Physical Review Letters* **97** 207205
[19] Bogart L K, Atkinson D, O'Shea K, McGrouther D and McVitie S 2009 *Physical Review B* **79** 054414
[20] García J M, Asenjo A, Velázquez J, García D and Vázquez M 1999 *Journal of Applied Physics* **85** 5480
[21] Cao H, Xu Z, Sang H, Sheng D and Tie C 2001 *Advanced Materials* **13** 121
[22] Bao J, Tie C, Xu Z, Ma Q, Hong J, Sang H and Sheng D 2002 *Advanced Materials* **14** 44
[23] Bao J, Xu D, Zhou Q, Xu Z, Feng Y and Zhou Y 2002 *Chemistry of Materials* **14** 4709-4713
[24] Rahman I Z, Boboc A, Razeeb K M and Rahman M A 2005 *Journal of Magnetism and Magnetic Materials* **290-291**, 246-249
[25] Zhan Q-F, Gao J-H, Liang Y-Q, Di N-L and Cheng Z-H 2005 *Physical Review B* **72** 024428
[26] Sun D-L, Gao J-H, Zhang X-Q, Zhan Q-F, He W, Sun Y and Cheng Z-H 2009 *Journal of Magnetism and Magnetic Materials* **321** 2737-2741
[27] Jaafar M, Serrano-Ramón L, Iglesias-Freire Ó, Fernández-Pacheco A, Ibarra M R, de Teresa J M and Asenjo A 2011 *Nanoscale Research Letters* **6** 407
[28] Asenjo A, Jaafar M, Navas D and Vazquez M 2006 *Journal of Applied Physics* **100** 023909
[29] Donahue M J and Porter D G 1999 National Technical Information Service Document No. PB99-163214, National Institute of Standards and Technology (NIST)
[30] Jaafar M, Gómez-Herrero J, Gil A, Ares P, Vázquez M and Asenjo A 2009 *Ultramicroscopy* **109** 693-699
[31] Iglesias-Freire Ó, Bates J R, Miyahara Y, Asenjo A and Grütter P H 2013 *Applied Physics Letters* **102** 022417